Environmental and Climate Technologies
2021, vol. 25, no. 1, pp. 600–609
https://doi.org/10.2478/rtuect-2021-0044
https://content.sciendo.com

Experimental Investigation and Prediction of Charging/Discharging Performance of Phase Change Material based Thermal Energy Storage Unit

Saulius PAKALKA[1*], Kęstutis VALANČIUS[2]

[1, 2] *Department of Building Energetics, Vilnius Gediminas Technical University, Sauletekio ave. 11, 10223 Vilnius, Lithuania*

[1] *Applied Research Institute for Prospective Technologies, Vismaliuku str. 34, 10243, Vilnius, Lithuania*

***Abstract* – The study presents the experimental and analytical investigation, which was carried out to evaluate the charging/discharging performance of phase change material (PCM) in the thermal energy storage (TES) unit. The experiments performed under different operating modes of the heat storage system, changing the inlet temperature and the mass flow rate of the heat transfer fluid (HTF). The calculated amount of thermal energy based on the partial enthalpy distribution provided by the manufacturer's datasheet compared to that obtained from the experiments. Based on the experimental results, a three-dimensional response surfaces formed and a regression models obtained, which allow predicting the PCM charging and discharging performance.**

***Keywords* – Charging/Discharging time; heat exchanger; phase change material (PCM); regression model; response surface**

Nomenclature		
PCM	Phase change material	–
HX	Heat exchanger	–
TES	Thermal energy storage	–
HTF	Heat transfer fluid	–
c_p	Specific heat capacity at constant pressure	J/(kgK)
$\dot{m}$	Mass flow rate	kg/s
m	Mass of phase change material	kg
$\dot{Q}$	Heat transfer rate	W
Q	Energy	J
Δh	Phase change enthalpy	J/kg
T	Temperature	°C
Subscripts		
1, 2, …	position No	–
AVG	average	–
CW	cold water	–

* Corresponding author.
E-mail address: saulius.pakalka@vilniustech.lt

©2021 Saulius Pakalka, Kęstutis Valančius.
This is an open access article licensed under the Creative Commons Attribution License (http://creativecommons.org/licenses/by/4.0).

HW	hot water	–
IN	inlet	–
OUT	outlet	–

1. INTRODUCTION

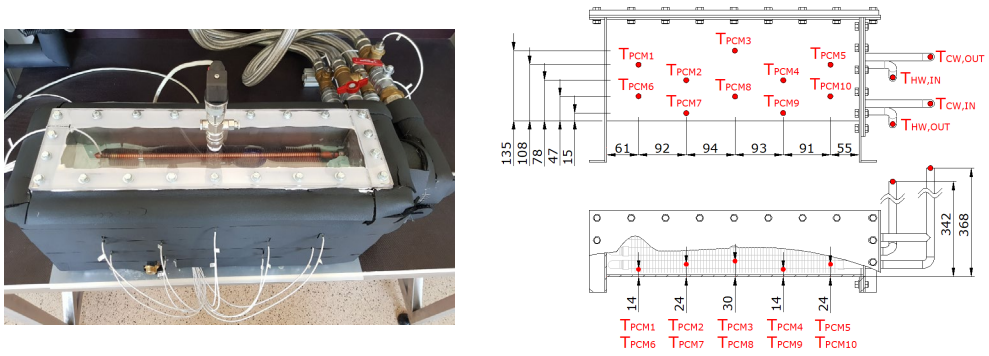
In order to design efficient and cost-effective phase change material (PCM) based thermal energy storage systems it is important to experimentally study their operation and apply the determined dependencies of parameters at the equipment design stage. In recent years, a lot of research [1], [2] has been carried out, setting different requirements and goals for them. PCMs of different types and different melting temperatures are investigated, numerical models are validated [3]–[5], the effect of technical solutions of thermal energy storage units, construction materials [6]–[9], heat transfer fluid flow rate and temperature [10], [11] on the system performance is analysed.

The obtained results are the basis for the improvement of the heat transfer process and the optimization of the operating modes of the PCM-based thermal energy storage unit. Therefore, it is important to determine how different factors and their combinations affect the phase transition process and predict the relationship between the operating factors (independent parameters) and responses (dependent parameters). For example, Yu *et al*. [12] conducted a study to determine the influence of PCM thermophysical properties on the charging process under steady and fluctuating heat source conditions and obtained a heat storage capacity and charging rate regression model. Yu *et al*. [13] performed optimization of the geometry of a shell-and-tube latent heat storage (LHS) unit with a tree-like fin using the response surface method (RSM). PCM melting duration selected as the objective response and length ratio and thickness index as the variables. Sciacovelli *et al*. [14] performed fin shape optimization of a shell-and-tube latent heat thermal energy storages (LHTES) unit through a combined use of numerical modelling and response surface method. The angle and length of the fin branches were chosen as design variables and the study found that the optimal fin design depends on the operating time of the LHTES unit.

The aim of this study is to compare experimentally obtained distribution of absorbed and released amount of heat with the manufacturer's declared partial enthalpy distribution in a given temperature range and to obtain regression models for PCM charging/discharging performance prediction. The experiments performed under different operation modes of the PCM based thermal energy storage (PCM-based TES) unit, changing the temperature and the mass flow rate of the supplied heat transfer fluid (HTF). The theoretical PCM heat storage capacity of the analysed PCM-based TES unit compared to the amount of heat absorbed and released during the experiment under different operating modes. Based on the experimental results a regression models are obtained, which allow predicting the PCM charging and discharging time.

2. EXPERIMENTAL SETUP AND METHODOLOGY

The subject of the study is a PCM-based TES unit with fin-and-tube type copper heat exchanger (PCM-HX) and organic PCM RT82 (Fig. 1). This PCM-HX designed to use in industrial waste heat recovery/storage systems within the temperature range of 90–100 °C. The analysed PCM-HX and PCM parameters presented in Table 1.



a) b)

Fig. 1. PCM-based TES unit with a copper heat exchanger (PCM-HX): (a) general view (b) positions of the temperature sensors (front and top view).

TABLE 1. PARAMETERS OF ANALYSED PCM BASED HEAT STORAGE UNIT

PCM heat exchanger		**Properties of PCM RT82 [15]**	
Fin quantity, units	79	Melting area, °C	77–82
Fin spacing, mm	5	Congealing area, °C	82–77
Fin thickness, mm	0.15	Heat storage capacity (±7.5 %), kJ/kg (combination of latent and sensible heat in a temperature range of 70 °C to 85 °C).	170
Tube diameter (OD), mm	12.7	Specific heat capacity, kJ/(kgK)	2
Tube thickness, mm	0.5	Density solid at 15 °C, kg/L	0.88
Heat exchanger weight, kg	2.1	Density liquid at 90 °C, kg/L	0.77
HX heat transfer area, m^2	1.75	Heat conductivity (both phases), W/(mK)	0.2
PCM weight, kg	4.34	Volume expansion, %	12.5
PCM volume solid/liquid, L	4.93/5.64	Max operation temperature, °C	100

The experimental setup employed in the present study made specifically for testing of PCM-based TES systems. Schematic representation of the experimental setup (test bench) is shown in Fig. 2. This experimental setup was also used and described in detail in previous studies [16]–[18].

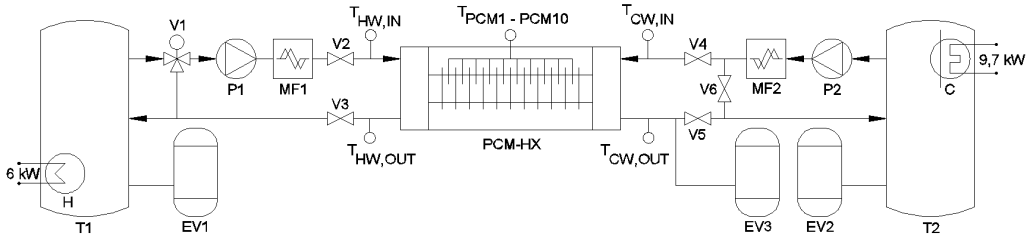


Fig. 2. Schematic representation of the experimental setup.

Fig. 2 shows the schematic drawing of the experimental setup, which consists of PCM based TES unit with copper HX (PCM-HX), temperature sensors (T_{PCM}, T_{HW} and T_{CW}), tanks for hot and cold water storage (T1, T2), expansion vessels (EV1, EV2, EV3), hot water heater (H), cold water cooler (C), mixing valve with electronic constant temperature controller (V1), manual valves (V2–V6), flowmeters (MF1, MF2) and circulating pumps (P1, P2).

The temperature of PCM (T_{PCM1}–T_{PCM10}), hot and cold water inlet ($T_{HW,IN}$, $T_{CW,IN}$) and outlet ($T_{HW,OUT}$, $T_{CW,OUT}$) was measured with PT100 temperature sensors (class B, accuracy ±(0.3 + 0.005 · t) °C). The water mass flow rate measured with flowmeters (MF1, MF2) (accuracy ± 0.15 %). Data logging interval – 1 Hz.

Experiments for this study carried out using different HTF (water) mass flow rates and different temperatures of inlet HTF (see Table 2). At the beginning of the charging (melting) cycle, PCM is in the solid phase at the temperature of about 30 °C. Hot water loop is opened (valves V2 and V3) and hot water at a set mass flow rate circulates through HX resulting in the charging of PCM. The charging cycle ends when the average PCM temperature is higher than 85.5 °C. At the beginning of the discharging (solidification) cycle, PCM is in the liquid phase at the initial temperature higher than 85.5 °C. Cold water loop is opened (valves V4 and V5) and cold water circulates through HX and PCM discharging begins. The solidification cycle ends when the temperature of the PCM becomes close to the temperature of the inlet HTF. The PCM-HX storage tank was thermally insulated by using 50 mm thick rock-wool and 4 mm thick closed cell elastomeric foam insulation. Due to the sufficient layer of thermal insulation, it is assumed that average power of thermal losses is negligible.

The heat capacity (ΔH) of PCM obtained by the following equation:

$$\Delta H = m \cdot \Delta h \,, \tag{1}$$

where

m Total mass of PCM, kg;

Δh Phase change enthalpy of PCM in a given temperature interval, J/kg.

The heat transfer rate ($\dot{Q}$) between the HTF (water) and the PCM was obtained by the following equation:

$$\dot{Q} = \dot{m} \cdot c_p \cdot dT \,, \tag{2}$$

where

$\dot{m}$ Mass flow rate of the heat transfer fluid, kg/s;

c_p Specific heat capacity at constant pressure, J/(kgK);

dT Temperature difference, K.

The amount of heat (Q) transferred during a time interval was determined based on the average rate of heat transfer into PCM and time step in given temperature intervals:

$$Q = \dot{Q} \cdot \Delta t \,, \tag{3}$$

where Δt is the time interval during which PCM temperature changes 1 °C, sec.

3. RESULTS AND DISCUSSION

The experiments performed using different HTF mass flow rate and inlet temperature. It is noticed that the PCM temperature varies unevenly at different measurement points, therefore it is assumed that the PCM temperature is uniform and was calculated as an average

temperature from 10 temperature sensors located at different positions in the PCM (see Fig. 1(b)). HTF mass flow rate is maintained constant throughout the charging/discharging process and inlet temperature is calculated as the average process temperature. The duration of the charging/discharging process at different operation modes obtained by integrating the time over the temperature range. The results presented in Table 2.

TABLE 2. OPERATION MODES

PCM charging (melting)				**PCM discharging (solidification)**			
Operation Mode #	$T_{HW,IN}$ °C AVG	ṁ, kg/s	Process duration, min	Operation Mode #	$T_{CW,IN}$ °C AVG	ṁ, kg/s	Process duration, min
MEL1	96.5	0.10	17.0	SOL1	20.8	0.10	5.02
MEL2	95.3	0.10	17.7	SOL2	19.6	0.10	4.85
MEL3	95.6	0.125	17.1	SOL3	28.9	0.125	5.35
MEL4	94.2	0.125	18.2	SOL4	30.1	0.125	5.48
MEL5	95.3	0.20	13.8	SOL5	23.5	0.20	4.50
MEL6	94.8	0.20	14.6	SOL6	22.5	0.20	4.48
MEL7	94.0	0.25	17.1	SOL7	26.9	0.25	4.55
MEL8	95.2	0.25	14.3	SOL8	28.3	0.25	4.82

Combined latent and sensible heat storage capacity of PCM RT82 in a temperature range of 70 °C to 85 °C is 170 kJ/kg ±7.5 % (see Table 1). The partial enthalpy distribution measured with 3-layer-calorimeter is provided in the manufacturer's data sheet [15]. Based on the above-mentioned temperature range stored energy as a function of temperature in given temperature intervals (step size 1 °C) was calculated for tested PCM mass (4.34 kg) and energy absorbed and released by the PCM during experiment at different operation modes was monitored. The results are shown in Fig. 3 and Fig. 4.

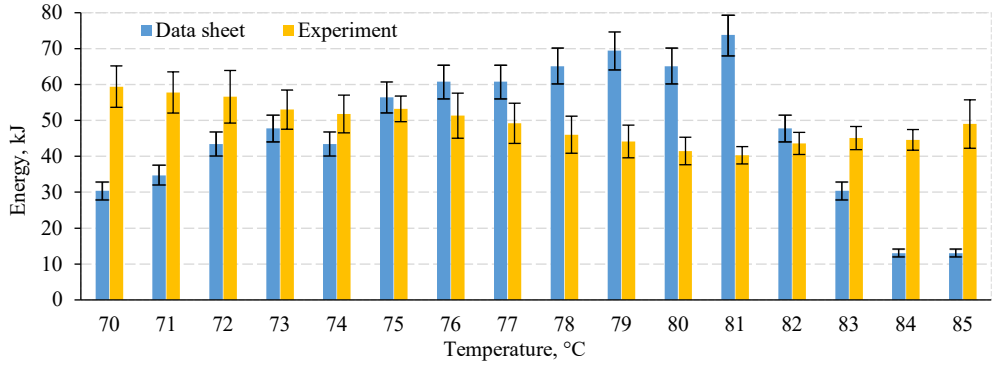


Fig. 3. Energy absorbed during PCM charging process (incl. standard deviation).

Fig. 3 shows the distribution of average stored heat in the PCM in a temperature interval of 1 °C. The experimental values were calculated as an average from 8 tested modes of charging process (MEL1 – MEL8). The temperature at which the maximum value of energy appears

corresponds to the melting temperature of the PCM. In the case of PCM RT82 this melting temperature interval is 77–82 °C and at this range highest values can be observed from calculation results based on data sheet. The distribution of stored heat in the case of experimentally obtained values differs from calculated ones and the standard deviation evaluates variation of stored energy depending on operating mode.

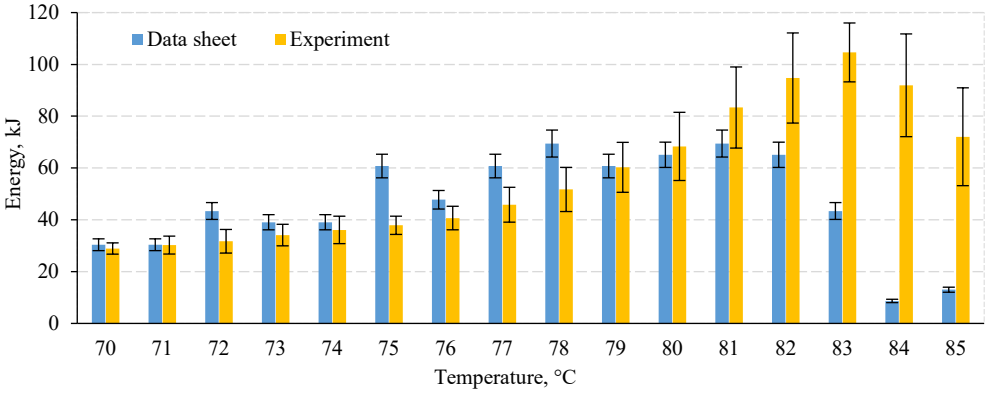


Fig. 4. Energy released during PCM discharging process (incl. standard deviation).

Fig. 4 shows the distribution of average released heat from the PCM in a temperature interval of 1 °C. The experimental values were calculated as an average from 8 tested modes of discharging process (SOL1 – SOL8). In the case of PCM RT82 the congealing area is 82–77 °C and from the graph can be seen that the maximum value of released heat appears in this region (Data sheet). Experimental data shows different distribution and highest values of released heat are observed from 81 °C to 84 °C. The amount of released energy varies depending on the test mode, and the standard deviation shows that the fluctuation is greater at higher temperatures.

Despite the different distribution of partial thermal energy which could be influenced by boundary conditions, it is important to compare total absorbed/released heat during entire temperature range (see Fig. 5).

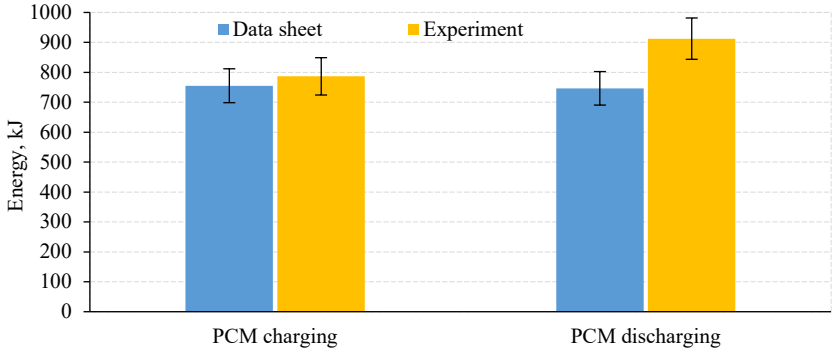


Fig. 5. Average stored energy during PCM charging and discharging processes (incl. standard deviation).

From Fig. 5 can be seen that in the case of PCM charging process experimentally obtained average value (787±62 kJ) are 4 % higher compared to calculated based on data sheet

(755±57 kJ). In the case of PCM discharging 22 % higher experimental value (913±69 kJ) is observed compared to calculated (746±56 kJ). However, after estimating the standard deviation, it can be stated that the average values of absorbed and released heat obtained from the declared PCM heat storage capacity and experiment vary within the error limits and can be used in further calculations. The obtained results also show that the average PCM temperature, according to which the calculations performed, is suitable for the evaluation of the amount of stored energy.

Based on the experimental results (Table 2) and using *Matlab Curve Fitting Toolbox* the regression models were derived (Eq. (4) and Eq. (5)). The second-order polynomial model used to predict the response. In the case of PCM charging determination coefficient $R^2 = 0.9468$ and adjusted $R^2 = 0.8758$. For the PCM discharging $R^2 = 0.9862$, adjusted $R^2 = 0.9679$.

The relationship between independent variables (HTF inlet temperature and mass flow rate) and response (PCM charging/discharging time) is shown in three-dimensional response surface plots (Fig. 6 and 7).

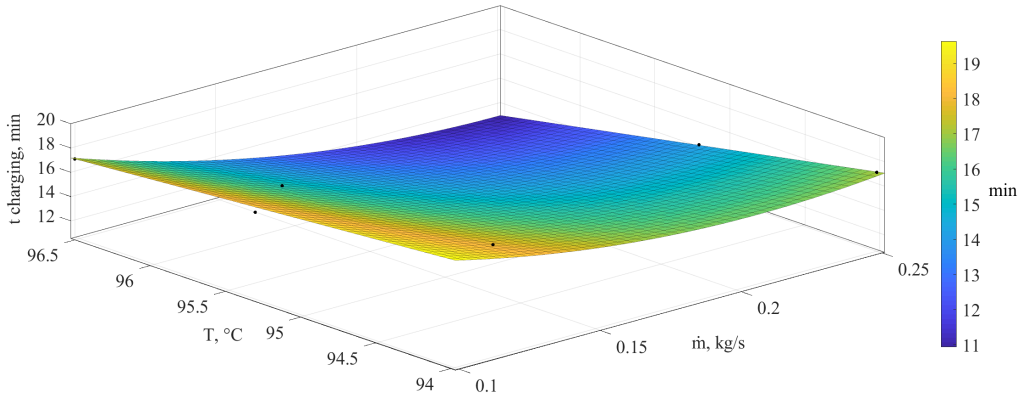


Fig. 6. Effect of HTF inlet temperature and mass flow rate on PCM charging time.

Fig. 6 shows the effect of HTF inlet temperature and mass flow rate on PCM charging time. The charging time increases with lower HTF inlet temperature as well as with low mass flow rate. Nevertheless, it should be noticed that even with higher mass flow rate and lower temperature, the charging time changes very slightly compared to lower flows. For example, Fig. 6 and Table 2 show that at an HTF flow of 0.1 kg/s and an inlet temperature of 96.5 °C, the PCM charging process took 17 min. When the HTF flow increased to 0.25 kg/s and the temperature reduced to 94 °C, the charging process time remained almost the same 17.1 min. This means that the HTF inlet temperature has a significantly greater effect on the duration of the process compared to the flow rate. This can be explained by the larger temperature difference between the heat exchanger and the PCM, which results in a higher heat transfer rate. PCM charging process equation describing the experimental points (coefficients with 95 % confidence bounds).

$$t_{\text{charging}} = 29.74 + 779.5 \cdot \dot{m} - 0.02023 \cdot T + 265.1 \cdot \dot{m}^2 - 9.46 \cdot \dot{m} \cdot T \tag{4}$$

Eq. (4) is valid for inlet HTF temperature range 94–96.5 °C and heat transfer rate 0.1–0.25 kg/s. Based on this regression model, it can be predicted that, for example, at a maximum HTF flow rate of 0.25 kg/s and a maximum temperature of 96.5 °C, the duration of the

charging process would be 11 min. Otherwise, at minimum temperature and flow rate, the estimated charging time would be 19.5 min.

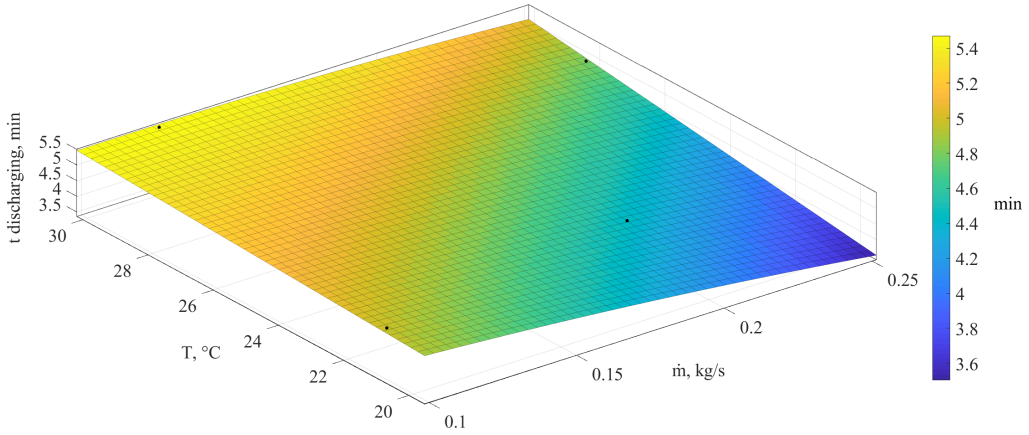


Fig. 7. Effect of HTF inlet temperature and mass flow rate on PCM discharging time.

Fig. 7 shows the effect of HTF inlet temperature and mass flow rate on PCM discharging time. The graph shows that at the lowest flow rate and highest temperature, the process duration is the highest and vice versa, the highest flow rate and the lowest temperature ensure the lowest process duration. This confirms the physics of heat transfer and according to Eq. (2) a larger temperature difference between HTF and PCM, as well as a higher HTF flow rate, ensures a higher heat transfer rate, which means a faster discharging process. It should be noticed, however, that HTF inlet temperature has a significantly greater effect on process duration than HTF mass flow rate. Comparing the different operation modes, in the case of SOL2 and SOL8 the process took 4.85 minutes and 4.82 minutes, respectively. Although the mass flow rate increased from 0.1 kg/s (SOL1) to 0.25 kg/s (SOL8), due to the 8.7 °C higher HTF inlet temperature the process duration was practically the same. PCM discharging process equation describing experimental points (coefficients with 95 % confidence bounds).

$$t_{\text{discharging}} = 5.366 - 12.95 \cdot \dot{m} - 0.006467 \cdot T - 22.66 \cdot \dot{m}^2 + 0.6018 \cdot \dot{m} \cdot T \tag{5}$$

Eq. (5) is valid for inlet HTF temperature range 20–30 °C and heat transfer rate 0.1–0.25 kg/s. Based on this regression model, it can be predicted that at a maximum HTF flow rate of 0.25 kg/s and a minimum temperature of 20 °C, the duration of the discharging process would be 3.6 min. Otherwise, at maximum temperature and minimum mass flow rate discharging time of 5.5 min is predicted. It should be noticed that in the case of discharging, both a shorter process and a smaller difference between the different operating modes are observed. The main reason for this is the larger temperature difference between HTF and PCM.

4. Conclusion

A method is presented to evaluate PCM stored energy based on partial enthalpy distribution and PCM average temperature. The experimental analysis shows that the amount of energy absorbed and released in a temperature range of 70 °C to 85 °C is close to the declared value in the PCM datasheet. Thus, based on the experimental data, the duration of the PCM

charging/discharging process determined under different operating modes and predictive models obtained.

Due to the smaller temperature difference between HTF and PCM, the charging process duration found to be on average 3.3 times longer compared to the discharging process. In addition, in the case of PCM discharging, the maximum difference between process duration of different operating modes is 1.0 minute, in the case of charging process – 4.4 minutes.

The regression models obtained during the study can be used to predict the PCM charging and discharging duration in similar configuration PCM-based TES units with fin-and-tube type copper heat exchanger depending on HTF mass flow rate and inlet temperature. The results are also important for optimization of the PCM-HX operation modes. Considering the energy consumption of the circulation pump, an optimal combination of parameters can be found to ensure the shortest charging/discharging process time at the lowest energy consumption.

REFERENCES

[1] Calderón A., *et al.* Where is Thermal Energy Storage (TES) research going? – A bibliometric analysis. *Solar Energy* 2020:200:37–50. https://doi.org/10.1016/j.solener.2019.01.050

[2] Nazir H., *et al.* Recent developments in phase change materials for energy storage applications: A review. *International Journal of Heat and Mass Transfer* 2019:129:491–523. https://doi.org/10.1016/j.ijheatmasstransfer.2018.09.126

[3] Zondag H. A., *et al.* Performance analysis of industrial PCM heat storage lab prototype. *Journal of Energy Storage* 2018:18:402–413. https://doi.org/10.1016/j.est.2018.05.007

[4] Zauner C., *et al.* Experimental characterization and simulation of a hybrid sensible-latent heat storage. *Applied Energy* 2017:189:506–519. https://doi.org/10.1016/j.apenergy.2016.12.079

[5] Dzikevics M., Veidenbergs I., Valančius K. Sensitivity Analysis of Packed Bed Phase Change Material Thermal Storage for Domestic Solar Thermal System. *Environmental and Climate Technologies* 2020:24:378–391. https://doi.org/10.2478/rtuect-2020-0022

[6] Mahdi J. M., Lohrasbi S., Nsofor E. C. Hybrid heat transfer enhancement for latent-heat thermal energy storage systems: A review. *International Journal of Heat and Mass Transfer* 2019:137:630–649. https://doi.org/10.1016/j.ijheatmasstransfer.2019.03.111

[7] Zayed M. E., *et al.* Recent progress in phase change materials storage containers: Geometries, design considerations and heat transfer improvement methods. *Journal of Energy Storage* 2020:30:101341. https://doi.org/10.1016/j.est.2020.101341

[8] Besagni G., Croci L. Experimental study of a pilot-scale fin-and-tube phase change material storage. *Applied Thermal Engineering* 2019:160:114089. https://doi.org/10.1016/j.applthermaleng.2019.114089

[9] Kabbara M., Groulx D., Joseph A. Experimental investigations of a latent heat energy storage unit using finned tubes. *Applied Thermal Engineering* 2016:101:601–611. https://doi.org/10.1016/j.applthermaleng.2015.12.080

[10] Nóbrega C. R. E. S., Ismail K. A. R., Lino F. A. M. Correlations for predicting the performance of axial finned tubes submersed in PCM. *Journal of Energy Storage* 2019:26:100973. https://doi.org/10.1016/j.est.2019.100973

[11] Mahdi M. S., *et al.* Numerical study and experimental validation of the effects of orientation and configuration on melting in a latent heat thermal storage unit. *Journal of Energy Storage* 2019:23:456–468. https://doi.org/10.1016/j.est.2019.04.013

[12] Yu X., *et al.* Sensitivity analysis of thermophysical properties on PCM selection under steady and fluctuating heat sources: A comparative study. *Applied Thermal Engineering* 2021:186:116527. https://doi.org/10.1016/j.applthermaleng.2020.116527

[13] Yu C., *et al.* Charging performance optimization of a latent heat storage unit with fractal tree-like fins. *Journal of Energy Storage* 220:30:101498. https://doi.org/10.1016/j.est.2020.101498

[14] Sciacovelli A., Gagliardi F., Verda V. Maximization of performance of a PCM latent heat storage system with innovative fins. *Applied Energy* 2015:137:707–715. https://doi.org/10.1016/j.apenergy.2014.07.015

[15] Rubitherm Technologies GmbH. Data sheet RT82 [Online]. [Accessed 20.01.2021]. Available: https://www.rubitherm.eu/media/products/datasheets/Techdata_-RT82_EN_09102020.PDF

[16] Pakalka S., Valančius K., Streckienė G. Experimental comparison of the operation of PCM-based copper heat exchangers with different configurations. *Applied Thermal Engineering* 2020:172:115138. https://doi.org/10.1016/j.applthermaleng.2020.115138

[17] Pakalka S., Valančius K., Streckienė G. Experimental and Theoretical Investigation of the Natural Convection Heat Transfer Coefficient in Phase Change Material (PCM) Based Fin-and-Tube Heat Exchanger. *Energies* 2021:14(3):716. https://doi.org/10.3390/en14030716

[18] Pakalka S., Valančius K., Damonskis M. Effect of Open and Closed Operation Modes on the Performance of Phase Change Material Based Copper Heat Exchanger. Presented at the *11th International Conference on Environmental Engineering*, Vilnius, Lithuania, 2020. https://doi.org/10.3846/enviro.2020.611